D/2

# N79-24013

## COMPARISON OF NASCAP PREDICTIONS WITH EXPERIMENTAL DATA

James C. Roche and Carolyn K. Purvis
NASA Lewis Research Center

## SUMMARY

NASCAP (the NASA charging analyzer program) is a three-dimensional, finite-element computer code capable of simulating the electrostatic charging of an arbitrary body either in a ground test tank or in the space environment. The code incorporates surface property parameters needed to simulate insulating and conducting materials. These parameters are being updated as required to bring the NASCAP predictions into correspondence with data from ground tests conducted at the Lewis Research Center. NASCAP predictions are also being compared with data from the ATS-5 spacecraft. The significance of these results is discussed.

## INTRODUCTION

In the past few years the electrostatic charging of spacecraft by the charged-particle environment has become an area of concern to both spacecraft designers and space scientists. This concern arises from the statistical correlation between the occurrence of electronic switching anomalies on spacecraft and the detection of geomagnetic substorm conditions by ground stations (ref. 1). The hypothesis is that this higher-energy-particle environment charges spacecraft surfaces to a point where breakdown occurs. The resulting electromagnetic interference is picked up by the spacecraft electrical wiring and triggers logic circuits, thereby causing the anomaly. Experimental and theoretical investigations have been established to test this hypothesis.

As usual, there are problems with both approaches. It is impossible to simulate completely the space environment in ground facilities. The usual compromise is to use energetic electrons (2 to 20 keV). Purely theoretical methods have been restricted to simplified cases involving equilibrium conditions or symmetrical geometry. A generalized digital computer simulation has a different set of strengths and weaknesses and could be used to complement both experiment and theoretical analysis. Clearly an analytical tool is needed to aid in the understanding of electrostatic charging phenomena.

Generalized digital computer simulations have been used in the past to solve complex body interactions, for example, thermal and structural analyzer computer codes such as SINDA (ref. 2) and NASTRAN (ref. 3). The NASA charging analyzer program (NASCAP) is a fully three-dimensional, Cartesian finite-element code with no symmetry or equilibrium restrictions. By taking time steps in a quasi-static manner, it can simulate the charging history of a general object either in space or in a test tank. However, the primary weakness of any finite-element approximation to a continuum is that fine-grain phenomena can occur between the finite number of lattice points into which the space is divided.

Accurate modeling of the surface interaction properties for the outer surface materials of an object is another problem that is common to both computer simulations and purely theoretical approaches. Near equilibrium, the net charging current to the object is the small difference between relatively large incoming and outgoing currents. The outgoing currents are due to such processes as backscattering, secondary emission, and photoemission. The models of these processes used in NASCAP were derived from the open literature. Parameter values for five common spacecraft surface materials (two conductors and three insulators) are included in the code.

This paper compares the NASCAP code computations with the results from a simple tank experiment. Also, by using a simulation of the ATS-5 spacecraft, comparisons are made between the predicted and actual potentials of the spacecraft structure. It is only through such comparisons that confidence can be built up in other, more complex, applications of the code.

## NASCAP CODE DESCRIPTION

The NASCAP code is a finite-element spacecraft-charging simulation that is written in FORTRAN V and is currently operational on two computers: the Univac 1100 at the Lewis Research Center and the CDC 6600 at the Air Force Geophysics Laboratory. An overall description of the code and its capabilities is given in reference 4. A detailed discussion of its physical basis is given in reference 5. The structure of the software itself is described in detail in reference 6.

### Program Elements

This description of the program elements is intended only as a brief survey to provide background information for this paper and is keyed to the flow chart in figure 1.

Environment definition. - One of two basic operating modes is specified: ground test tank or space. For the ground-test mode, the outer boundary of the computational grid is grounded and an electron beam of an arbitrary current-density pattern is aimed along the central axis. For the space mode, a plasma environment is specified at the outer boundary - either pure Maxwellian or an arbitrary distribution. For either case the direction and magnitude of the incident solar illumination is specified.

Object definition. - The object to be defined and the space immediately adjacent to it are divided into a number of volume cells (referred to as the inner grid) from 16x16x16 to 16x16x32. The object is modeled by using cubical cells and such portions of these cells as can be constructed by sectioning cubes (fig. 2). There can be as many as 1000 surface cells, each of which can either be covered with an insulating film or left bare. The number of nested grids (fig. 3) is then specified, each of which has twice the size and half the resolution of the next inner grid. For example, an inner grid plus two nested grids would contain from 13 000 to 26 000 computational points.

Trajectory calculations. - Starting from a known particle flux at the outer boundary and an assumed initial potential, the incident flux to each surface cell is computed.

Shadowing. - Starting from the known solar vector, the percentage of illumination that falls on each surface cell is computed.

Surface interactions. - Starting from known particle and photon fluxes on each surface cell, the backscattering secondary emission and photoemission are computed. Surface materials and their interaction processes are modeled by using the following list of parameters (table I):

(1) Relative dielectric constant

(2) Thickness of dielectric film

(3) Electrical conductivity

(4) Atomic number

(5) Maximum secondary-electron yield for electron impact at normal incidence

(6) Primary-electron energy to produce maximum yield at normal incidence

(7-10) Four empirical parameters for use in a double-exponential model of penetration depth of incident electrons (range)

(11) Secondary-electron yield for normally incident 1-keV protons

(12) Proton energy to produce maximum secondary-electron yield

(13) Photoelectron yield for normally incident sunlight

The atomic number is used in the computation of back-scattered electrons and also, if required, in the Feldman range formula (table I, footnote c). The range is used in the computation of secondaries due to primary electrons. The values of all these parameters for five materials as initially incorporated into the NASCAP code are given in reference 6 and are repeated here in table I.

Charge accumulation. - The net current to each surface cell is determined and assumed to hold constant over one time increment. This results in an updated charge pattern over the surface of the test object.

Potential solver. - Given the updated charge pattern on the surface of the object, the potential solver uses a conjugate gradient iteration method to compute the potentials at each grid point. These new potentials can now be used to compute new fluxes to each cell for the next time step.

## OPERATING CONDITIONS

A few words are in order regarding the computer running time for these simulations. The tank model, for example, has 22 000 grid points and required about 13 seconds of computer time for each potential iteration. NASCAP prints out a numerical measure of convergence, and it is possible to inspect this parameter and judge the appropriate number of iterations for each time step. A method for automatically adjusting the number of iterations so that the potential converges to within some specified accuracy is being incorporated into the code. The length of the time step and the accuracy could then be selected according to the physical situation with the knowledge that the number of potential iterations will adjust itself to meet these constraints.

For space-mode calculations the current version of NASCAP is capable of handling spacecraft that are three-axis stabilized or slowly spinning. A rapidly spinning spacecraft in sunlight is difficult to simulate. This case is discussed in more detail in the section Summary of ATS-5 Comparison. A method of applying average levels of illumination to the appropriate cells on a constant basis will be incorporated into the code to handle rapidly spinning spacecraft in sunlight.

## COMPARISON OF NASCAP PREDICTIONS WITH GROUND-TEST DATA

In ground-test-tank experiments, material specimens are exposed to the flux from an electron gun. Therefore only those properties of the material that are related to electron impact, such as backscattered electrons and secondary-electron emission, are relevant. Comparing NASCAP predictions with test data would then verify the electron-impact material parameters. This leaves the parameters related to proton impact yet to be evaluated. This could be accomplished by space flight data comparisons.

### Procedure

The test-tank experiments used for comparison with NASCAP predictions were conducted in a 2-meter-diameter vacuum chamber at the Lewis Research Center. Flat test specimens were irradiated with an electron beam, and their surface voltages were monitored with a field-sensing probe that scans across the surface at regular intervals at a distance of 3 millimeters. Before each experiment, the surface of the specimen was discharged with a plasma source. This facility and its instrumentation are described in detail in reference 7.

The NASCAP model of this facility is shown in figure 3. The cylindrical tank is modeled by the square cross-section of the third and outer grid, which is truncated at each end to the correct length. There are a total of approximately 22 000 grid points in this relatively simple model. The test specimen has a cross-section of 15 centimeters by 20 centimeters and is located, as shown, in the inner grid. The resolution in the test specimen is 2.5 centimeters. The electron beam is aimed along the central axis of the tank. Since NASCAP is capable of modeling an arbitrary current-density pattern, data from an electron gun calibration were inserted into the code. After a slight beam curvature - caused by the magnetic field of the Earth - is allowed for, the gun current-flux profile is taken to be that which would produce the measured current-density pattern in the plane of the test specimen before any charging. As the specimen charges, the current-density pattern spreads, but the flux profile at the gun remains constant.

Tests were conducted on the following types of specimens: bare aluminum baseplate, silvered Teflon (0.127 mm thick), two types of thermal blanket, and a solar-array-segment module. The thermal blankets both consisted of a surface layer of Kapton (0.127 mm thick) over multiple layers of silvered Mylar that were grounded to the baseplate. The blankets differed only in the technique used for grounding the Mylar layers. The aluminum baseplate was grounded for all tests except the first, in which it was left bare and ungrounded so that its floating potential could be measured. Each specimen was irradiated with a beam having a nominal central density of 1 $nA/cm^2$ as measured with a Faraday cup. The beam accelerating voltage was set at 5, 8, 10, and 12 keV for each specimen.

The silvered Teflon was modeled as a plain, 0.127-millimeter-thick layer of Teflon since it was bonded to the baseplate with the silvered side against the plate. Both thermal blankets were modeled as a 0.127-millimeter-thick layer of Kapton since this was the composition of the top layer of both blankets and the metallized layers underneath were grounded. The solar-array-segment module was modeled as a 0.203-millimeter-thick layer of silica.

## Summary of Ground-Test Comparisons

Surface voltage profiles for the test samples, resulting from electron bombardment, were compared with the NASCAP predictions by using the available literature values for electron-impact material parameters (table I). The results are summarized here.

<u>Aluminum</u>. - The NASCAP comparison indicated that the aluminum test surface was, in reality, an aluminum oxide surface. Using literature values for the material properties of aluminum oxide instead of pure aluminum resulted in excellent agreement (fig. 4). Since no special precautions were taken to prevent oxidation of the aluminum, it is reasonable to assume that the test surface was aluminum oxide.

Only the steady-state potentials were compared for this specimen. To compare transient surface voltages, the NASCAP code requires a value for the capacitance between the electrically floating aluminum plate and ground. This capacitance value was not available.

<u>Silvered Teflon</u>. - The steady-state NASCAP predictions for silvered Teflon are in excellent agreement with the test data (fig. 5). The transient voltage predictions are in fair agreement but seem to lag consistently behind the experimental charging data.

<u>Aluminized Kapton</u>. - Both the steady-state and transient predictions for aluminized Kapton are in good agreement with the limited test data (fig. 6).

<u>Solar-array segments</u>. - There are significant discrepancies between the predictions and the test data for solar-array (silicon dioxide) segments (fig. 7). The difficulty here could be similar to that which was experienced with the bare aluminum plate. The solar-array cover slide that was tested had a coating of an antireflective compound, but the parameters in table I were derived for pure silica. This case is still under investigation, and parameter adjustments will be made when additional data are available.

## COMPARISON OF NASCAP PREDICTIONS WITH ATS-5 DATA

The spacecraft that was selected for comparison with the NASCAP code was the ATS-5. This spacecraft carries a particle analyzer, and thus there is a large amount of information available concerning its charged-particle environment. Information on the spacecraft itself and its instruments is given in reference 8. Data from its particle analyzer have been reduced and fitted to a double Maxwellian model (ref. 9).

### Procedure

The NASCAP model of the ATS-5 is shown in figure 8. The cylindrical outer surface of the spacecraft is modeled as an octagon with a central region covered with Teflon and end regions covered with silica to simulate the solar array. The cavities at each end are covered with Teflon. Since about 10 percent of the solar-array area consists of exposed metallic interconnects, 10 percent of the surface cells in the solar-array regions have been left as exposed aluminum. There are 880 surface cells in this model. The environment was simulated by a single Maxwellian approximation with a density of 1 particle per cubic centimeter and a temperature of 5 keV for both species. These values are typical of much of the actual data.

### Summary of ATS-5 Comparison

First, eclipse conditions were simulated by using parameters from table I. This resulted in a spacecraft ground potential of approximately -2300 volts, which did not agree with the flight data. However, the simple expedient of halving the secondary yields due to ion impact on the Teflon and the silica (which are not well-known values) produced a spacecraft ground potential of -3800 volts, a figure that was actually measured on the spacecraft several times under similar environmental conditions. Figure 9 shows potential contours in the charged condition (spacecraft ground at -3800 V).

The ATS-5 rotated at 76 revolutions per minute. As noted earlier, a rapid spin rate presents a practical simulation problem. NASCAP models the rotation by changing the Sun angle and recomputing the shadow pattern at each time step. For this to be a realistic simulation, there should be at least 10 time steps per revolution, or approximately 80-millisecond time steps. Although absolute charging occurs in a matter of seconds, it takes many minutes for the differential charging pattern to fully develop. This would lead to a prohibitive number of time steps.

If the spin rate is reduced so that larger time steps can be taken, another problem is encountered: saddle-point formation (ref. 10). This saddle-point formation results from a field distribution around the satellite that effectively reduces photocurrents from the illuminated surfaces. This limits the NASCAP treatment of rapidly spinning spacecraft. This constraint will be alleviated in future modifications of the code.

A simulation of a stationary ATS-5 model in the sunlight was run for qualitative comparison only. The resulting potential contours are shown in figure 10 and seem to be reasonable. The simulation indicated a ground potential from -400 to -500 volts. Flight data from the spinning ATS-5 have shown ground potentials near zero volts in the sunlight. Therefore, it seems plausible that a stationary ATS-5 that is having a fraction of its electron emission suppressed by a saddle point on its sunlit side would develop such negative potentials.

## CONCLUDING REMARKS

The work described herein demonstrates that the NASCAP code generates results that are in reasonable agreement with available ground-test and spacecraft data. Ground-test results reveal that better material-property values are needed for the five common materials currently implemented in the code. Altering the values of the code parameters is a simple task, and the code is structured so that even the models of the processes could be changed without disrupting other areas of the code. Also, a methodical system for altering the values of the code parameters in response to experimental data is clearly needed.

## REFERENCES


1. McPherson, D. A.; Cauffman, D. P.; and Schober, W.: Spacecraft Charging at High Altitudes - The SCATHA Satellite Program. AIAA Paper 75-92, Jan. 1975.

2. Smith, J. P.: Systems Improved Numerical Differencing Analyzer (SINDA): User's Manual. TRW-14690-H001-R0-00, TRW Systems Group, 1971.

3. The NASTRAN User's Manual (Level 16.0 Supplement). NASA SP-222(03), 1976.

4. Katz, I.; et al.: The Capabilities of the NASA Charging Analyzer Program. Spacecraft Charging Technology - 1978. NASA CP-2071, 1979.

5. Katz, I.; et al.: A Three Dimensional Dynamic Study of Electrostatic Charging in Materials. (SSS-R-77-3367, Systems Science and Software; NASA Contract NAS3-20119.) NASA CR-135256, 1977.

6. Mandell, M. J.; Harvey, J. M.; and Katz, I.: NASCAP User's Manual. (SSS-R-77-3368, Systems Science and Software, NASA Contract NAS3-20119.) NASA CR-135259, 1977.

7. Berkopec, F. D.; Stevens, N. J.; and Sturman, J. C.: The Lewis Research Center Geomagnetic Substorm Simulation Facility. NASA TM X-73602, 1976.

8. Goldstein, R.; and DeForest, S. E.: Active Control of Spacecraft Potentials at Geosynchronous Orbit. Spacecraft Charging by Magnetospheric Plasmas, Progress in Astronautics and Aeronautics. Vol. 47, A. Rosen, ed., American Institute of Aeronautics and Astronautics, 1976, pp. 169-181.

9. Garrett, H. B.: Modeling of the Geosynchronous Orbit Plasma Environment - Part I. AFGL-TR-77-0288, Pt. 1, Air Force Geophysics Laboratory, 1977.

10. Mandell, M. J.; et al.: The Decrease in Effective Photocurrents due to Saddlepoints in Electrostatic Potentials near Differentially Charged Spacecraft. Presented at the 1978 IEEE Annual Conference on Nuclear and Space Radiation Effects, Albuquerque, N. Mex., July 18-21, 1978, Session C-4.

TABLE I. - MATERIAL-PARAMETER VALUES

| Parameter | Description | Material | | | | |
|---|---|---|---|---|---|---|
| | | Aluminum | Magnesium | Teflon | Kapton | Silica |
| 1 | Relative dielectric constant (dimensionless) | 1.0 | 1.0 | 2.0 | 3.5 | 4.0 |
| 2 | Thickness of dielectric film, m | (a) | (a) | (a) | (a) | (a) |
| 3 | Electrical conductivity, mho/m | [b]-1 | [b]-1 | $10^{-14}$ | $10^{-14}$ | $10^{-14}$ |
| 4 | Atomic number (dimensionless) | 13 | 12 | 10 | 5 | 10 |
| 5 | Maximum secondary-electron yield for electron impact at normal incidence (dimensionless) | 0.97 | 0.92 | 3.00 | 2.10 | 2.40 |
| 6 | Primary-electron energy to produce maximum yield at normal incidence, keV | 0.30 | 0.25 | 0.30 | 0.15 | 0.40 |
| 7-10 | Parameters used in double-exponential model: dimensionless | 26 | [c]-1 | [c]-1 | [c]-1 | 25 |
| | ------------ | 1.30 | ---- | ---- | ---- | 0.12 |
| | dimensionless | 24 | (1.74) | (2.00) | (1.42) | 36 |
| | ------------ | 1.73 | (24.3) | (16.7) | (9.8) | 1.63 |
| 11 | Secondary-electron yield for normally incident 1-keV protons (dimensionless) | 1.36 | 1.36 | 1.40 | 1.40 | 1.40 |
| 12 | Proton energy to produce maximum secondary-electron yield, keV | 40 | 40 | 70 | 70 | 70 |
| 13 | Photoelectron yield for normally incident sunlight | $4\times10^{-5}$ | $2\times10^{-5}$ | $2\times10^{-5}$ | $2\times10^{-5}$ | $2\times10^{-5}$ |

[a]As required.

[b]A flag indicating a vacuum gap over a bare conductor.

[c]A flag indicating the use of Feldman's range formula (ref. 1, appendix F.2). After receipt of this flag, the eighth parameter is ignored, the ninth parameter is specific gravity, and the tenth parameter is mean atomic weight.

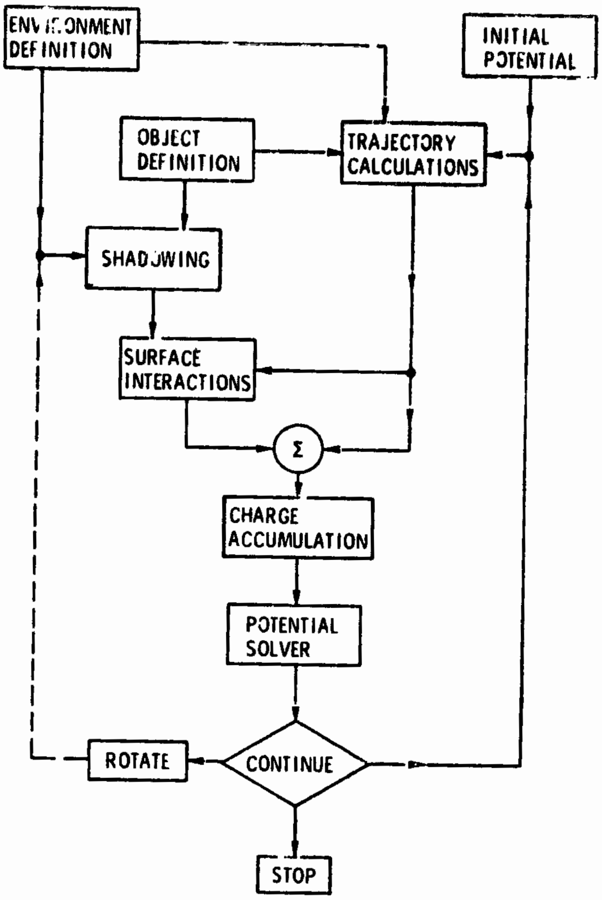


Figure 1. - NASCAP flow chart.

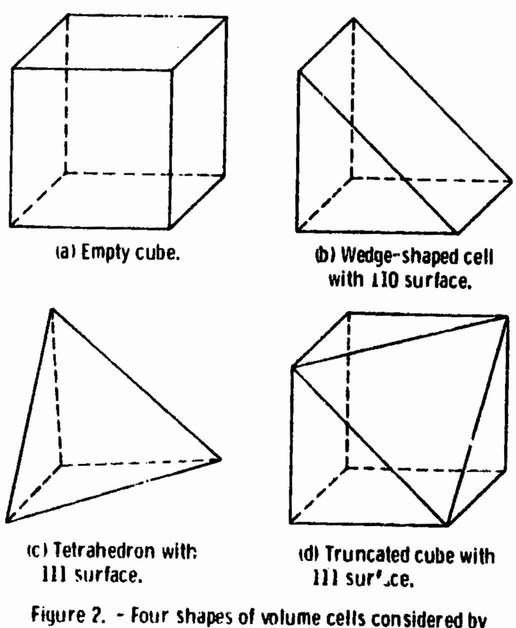

(a) Empty cube.

(b) Wedge-shaped cell with 110 surface.

(c) Tetrahedron with 111 surface.

(d) Truncated cube with 111 surface.

Figure 2. - Four shapes of volume cells considered by NASCAP code.

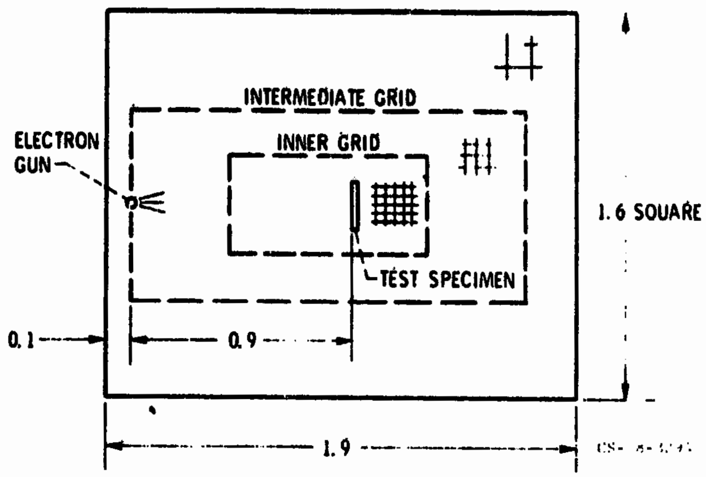


Figure 3. - Test-tank model. (Dimensions are in meters.)

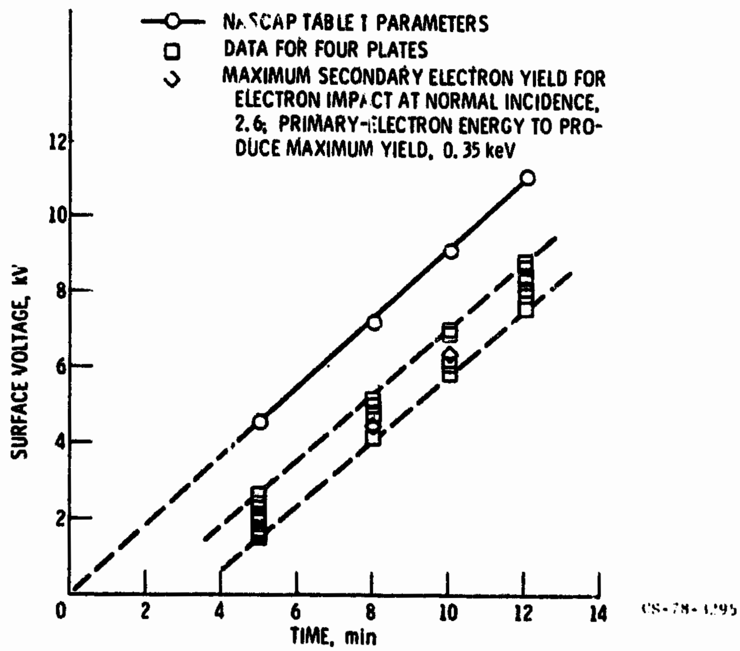


Figure 4. - Surface voltage profile for aluminum.

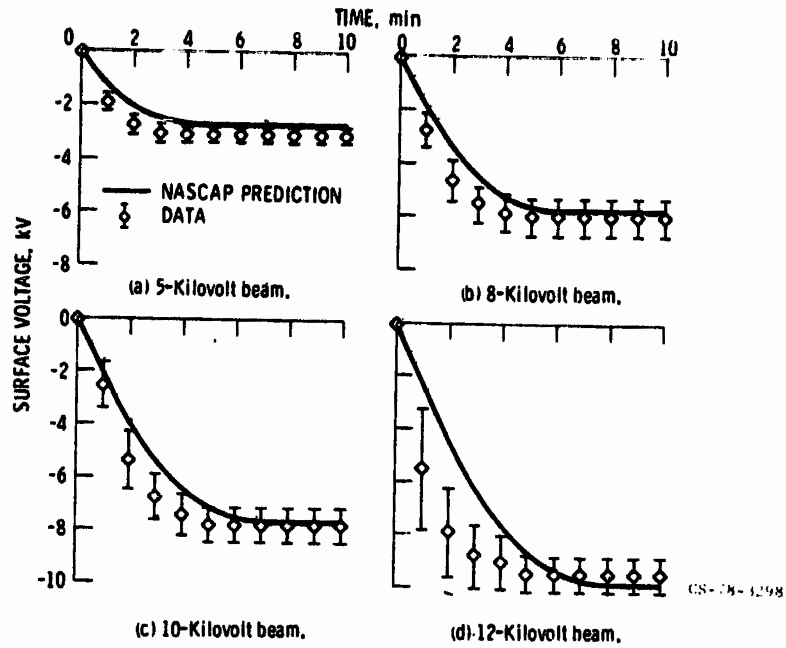


Figure 5. - Surface voltage profiles for silvered Teflon.

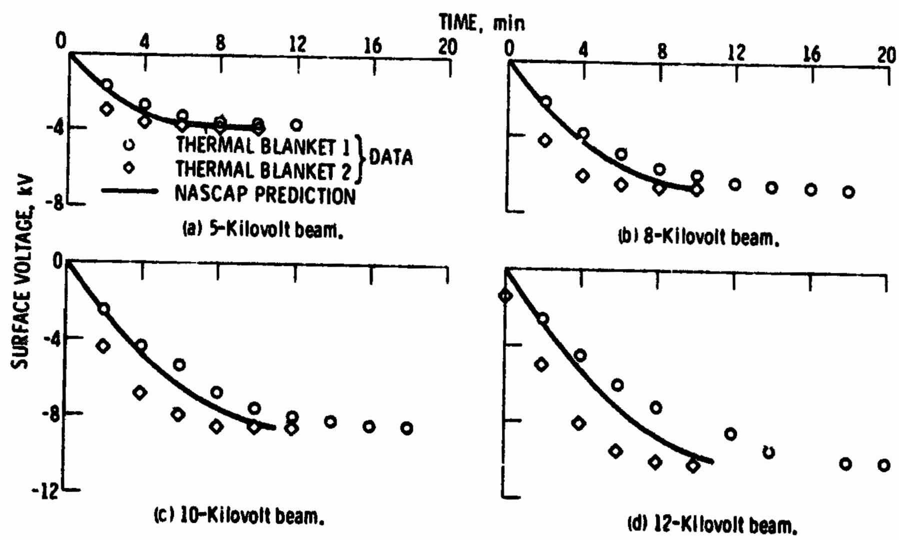


Figure 6. - Surface voltage profiles for aluminized Kapton.

CS-78-1299

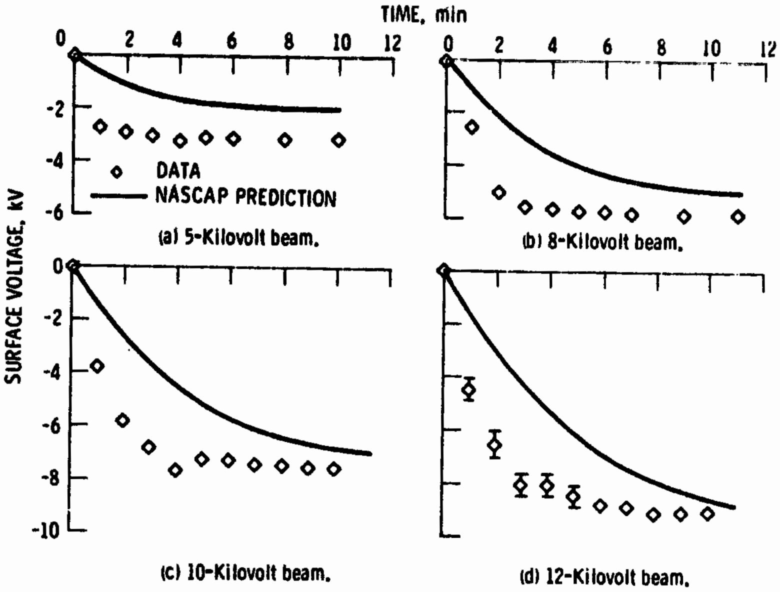


Figure 7. - Surface voltage profiles for solar-array (silicon dioxide) segments.

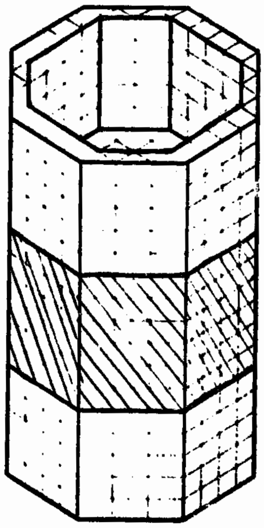

CS-78-3293

Figure 8. - NASCAP model of ATS-5.

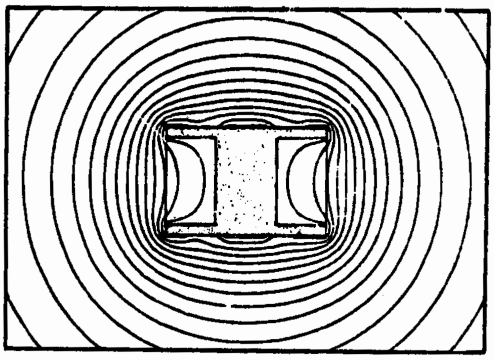

Figure 9. - Simulation of potential contours of ATS-5 in charged condition in eclipse.

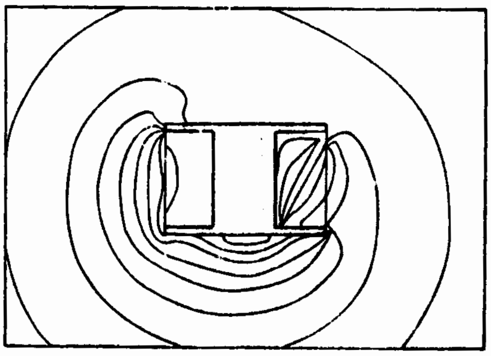

Figure 10. - Simulation of potential contours of ATS-5 in sunlight.